



Article

Comprehensive Assessment of BDS-2 and BDS-3 Precise Orbits Based on B1I/B3I and B1C/B2a Frequencies from iGMAS

Zhetao Zhang , Ping Zeng, Yuanlan Wen *, Lina He and Xiufeng He

School of Earth Sciences and Engineering, Hohai University, Nanjing 211100, China

* Correspondence: wwwgwyl@126.com; Tel.: +86-135-4968-7989

Abstract: The BeiDou Global Navigation Satellite System (BDS), including the second generation (BDS-2) and the third generation (BDS-3), has been widely used in areas of positioning, navigation, and timing (PNT). One of the essential prerequisites for accurate PNT service is the precise satellite orbits of multi-frequency and multi-constellation BDS-2 and BDS-3 satellites. As usual, the precise orbit products can be obtained from analysis centers (ACs) of the international GNSS Service (IGS). The precise orbits can also be downloaded from the international GNSS Monitoring and Assessment System (iGMAS). Compared with the IGS ACs, the iGMAS can provide featured services such as satellite orbits based on the new B1C/B2a BDS signals. Considering the indispensability of the new signals, the performance of all BDS precise orbits from iGMAS needs to be known. However, there is no comprehensive assessment of BDS-2 and BDS-3 precise orbits based on B1I/B3I and B1C/B2a frequencies from iGMAS, especially for the period after the BDS entered the stable operation stage. In this paper, BDS-2/BDS-3 final (ISC), rapid (ISR), and ultra-rapid (ISU) products based on B1I/B3I and B1C/B2a frequencies from iGMAS are all assessed comprehensively. Specifically, at first, the precise orbits from iGMAS are compared with the ones from the IGS ACs. Based on this, the satellite laser ranging inspects the precise orbits from iGMAS. Finally, the orbit errors are discussed systematically by considering the beta and elongation angles. Using one year of data, the orbit accuracy of geostationary orbit, inclined geosynchronous orbit, and medium earth orbit (MEO) satellites can almost reach meter to decimeter level, decimeter to sub-decimeter level, and centimeter level, respectively, where the ISC products are the best. The ISC, ISR, and ISU products based on B1I/B3I frequencies are generally better than the ones based on B1C/B2a frequencies. Additionally, according to the SLR data, the results show that the accuracy of precise orbits of BDS-3 is better than that of BDS-2. The mean values of orbit biases of BDS-3 MEO satellites are approximately 2.88 cm. In addition, the orbit errors are related to the beta angle and elongation angle to some extent, and the manufacturers may also have an influence on the orbit errors.

Keywords: BDS; B1I/B3I frequencies; B1C/B2a frequencies; iGMAS; precise orbits



Citation: Zhang, Z.; Zeng, P.; Wen, Y.; He, L.; He, X. Comprehensive Assessment of BDS-2 and BDS-3 Precise Orbits Based on B1I/B3I and B1C/B2a Frequencies from iGMAS. *Remote Sens.* **2023**, *15*, 582. <https://doi.org/10.3390/rs15030582>

Academic Editor: Andrzej Staszczak

Received: 10 December 2022

Revised: 14 January 2023

Accepted: 14 January 2023

Published: 18 January 2023



Copyright: © 2023 by the authors. Licensee MDPI, Basel, Switzerland. This article is an open access article distributed under the terms and conditions of the Creative Commons Attribution (CC BY) license (<https://creativecommons.org/licenses/by/4.0/>).

1. Introduction

Up to now, the BeiDou Navigation Satellite System (BDS) has been completed. It has been put into use in areas of positioning, navigation, and timing (PNT), which includes the second-generation one (BDS-2) and third-generation one (BDS-3) [1,2]. The BDS is a multi-source heterogeneous constellation with three types of satellites and five frequencies in total. Specifically, according to the China Satellite Navigation Office (CSNO), the three types of satellites are geostationary orbit (GEO), inclined geosynchronous orbit (IGSO), and medium earth orbit (MEO) satellites, respectively. The five available frequencies are B1C (1575.420 MHz), B1I (1561.098 MHz), B3I (1268.520 MHz), B2b/B2I (1207.140 MHz), and B2a (1176.450 MHz) signals, respectively [3–7]. As of December 2022, there are 15 BDS-2 satellites in orbit, including five GEO, seven IGSO, and three MEO satellites, respectively. For BDS-3 satellites, there are 29 BDS-3 satellites in total, consisting of two GEO, three IGSO, and 24 MEO satellites in orbit [8]. Moreover, the BDS-2 GEO/IGSO/MEO and

BDS-3 GEO/IGSO satellites are manufactured by the China Academy of Space Technology (CAST), and BDS-3 MEO satellites are built by the CAST or Shanghai Engineering Center for Microsatellites (SECM). Apparently, obtaining the precise satellite orbits of BDS-2 and BDS-3 satellites is the prerequisite of high-precision and high-reliability PNT service [9].

As usual, global navigation satellite system (GNSS)-related products can be obtained from the international GNSS Service (IGS), including satellite orbits, clock corrections, Earth rotation parameters, geocentric coordinates of IGS tracking stations, and tropospheric and ionospheric parameters [10]. Currently, twelve IGS analysis centers (ACs) can provide related precise products [11]. Specifically, they are Natural Resources Canada (EMR), Wuhan University (WHU), Geodetic Observatory Pecny (GOP), Space geodesy team of the CNES (GRG), European Space Agency (ESA), GeoForschungsZentrum (GFZ), Center for Orbit Determination in Europe (CODE), Jet Propulsion Laboratory (JPL), Massachusetts Institute of Technology (MIT), National Geodetic Survey (NGS), Scripps Institution of Oceanography (SIO), and U.S. Naval Observatory (USNO). Recently, the Multi-GNSS Experiment (MGEX) has been set up and can provide multi-GNSS, including global positioning system (GPS), GLONASS (GLObal'naya NAVigatsionnaya Sputnikovaya Sistema), Galileo, and BDS products [12,13], etc. Many scholars have analyzed the four-system orbit and clock products provided by MGEX ACs [14–17]. However, it is worth noting that one may combine the above products from different ACs to improve reliability in real applications [18].

To further monitor and assess the performance and status of BDS-2 and BDS-3, the international GNSS Monitoring and Assessment System (iGMAS) has been established [19,20]. As of December 2022, the iGMAS has 30 tracking stations, three data centers, and 12 ACs. The 12 ACs include Xi'an Satellite Control Center, Shanghai Astronomical Observatory, Information Engineering University, Beijing Aerospace Control Center, Chinese Academy of Surveying and Mapping, Innovation Academy for Precision Measurement Science and Technology, Chang'an University, Wuhan University, National Time Service Center, China University of Mining and Technology, Xi'an Research Institute of Surveying and Mapping, and Tongji University [21]. Based on the observed multi-frequency and multi-constellation GNSS observations, including BDS, GPS, GLONASS, and Galileo collected by the tracking stations, the ACs obtain the multi-GNSS data from data centers and generate the precise products, including satellite orbits, clock corrections, Earth rotation parameters, geocentric coordinates of iGMAS tracking stations, and tropospheric and ionospheric parameters, etc. Based on the products from different ACs, the iGMAS will combine and generate the final (ISC), rapid (ISR), and ultra-rapid (ISU) orbit products. Therefore, the iGMAS can promote compatibility and interoperability among different GNSS constellations [16,22]. One of the most notable features of iGMAS is that it supports new BDS signals B1C/B2a and related products.

Since the orbit products will directly affect the PNT performance and other related applications [23–25], assessing the precision and reliability of the iGMAS orbit products at hand is crucial. At earlier times, compared with the IGS products, the precision of BDS-2 GEO/IGSO and MEO satellites from iGMAS is better than 10 cm and approximately 1 m, respectively [26]. Later, several studies show that by using the iGMAS products, the precision of BDS-3 IGSO and MEO satellites is approximately 10 cm and 40 cm [27], which somewhat shows improvements. To further evaluate the BDS products from iGMAS, the satellite-induced code pseudorange variation [28], differential code bias [29], and signal quality [30] are studied. In addition, the satellite laser ranging (SLR) data are applied to validate the BDS-2 precise orbits [31]. Actually, since the middle of 2019, the iGMAS has been the only center that can provide the orbit products based on B1I/B3I and B1C/B2a signals simultaneously. In contrast, the others can only offer the ones of B1I/B3II signals. Recently, the latest research found the potential advantage of B1C/B2a signals compared with the B1I/B3I signals, such as in better signal-in-space range error [32]. In theory, the B1C/B2a-based orbit products are advised when using the B1C/B2a signals for better consistency. Therefore, it is indispensable to systematically evaluate all kinds of BDS products from iGMAS.

Unfortunately, to our best knowledge, there is no comprehensive assessment of BDS-2 and BDS-3 precise orbits based on B1I/B3II and B1C/B2a frequencies from iGMAS, especially for the period after the BDS entered the stable operation stage. In this paper, all kinds of BDS products are systematically studied, where the BDS-2/BDS-3 ISC, ISR, and ISU precise orbit products based on B1I/B3I and B1C/B2a frequencies from iGMAS are all included. Specifically, to comprehensively evaluate the different orbits of iGMAS, the MGEX precise orbits from four primary ACs that can provide BDS orbits, particularly the BDS-3, are used for orbit comparison. Secondly, the optical technique of SLR is used as an external independent validation for the radial components of iGMAS products. Thirdly, the orbit errors from iGMAS are discussed in depth, where the influential factors including beta angle and elongation angle are considered.

2. Methodology

To evaluate the precise orbits of iGMAS, the first strategy is to compare the products of iGMAS with those of other ACs, such as GFZ, ESA, CODE and WHU, etc. Whereas the product difference can only depict the consistency between two arbitrary agencies, new products, such as precise orbits based on B1C/B2a frequencies, cannot be assessed with high accuracy and high reliability. Therefore, the SLR residuals are further applied to inspect the precise orbits of iGMAS, where the B1I/B3I and B1C/B2a are included.

The inspection with SLR residuals is actually the differences between the computed satellite-to-receiver range with precise products and the observed SLR observations. The SLR observation equation can be expressed as follows [33]:

$$\rho_{SLR} = \frac{1}{2}c\tau + d_t + d_{sr} + d_{td} + d_{pm} + \epsilon \quad (1)$$

where ρ_{SLR} denotes the SLR observation; c and τ denotes the light speed in a vacuum and the time interval from laser emission to reception; the d_t , d_{sr} , d_{td} , d_{pm} and ϵ denote the time offset, station-specific range bias, tidal displacement correction of site position, plate motion correction of the station, and other observation error, respectively. Here, the ϵ mainly includes the center-of-mass correction, tropospheric delay, space-time curvature correction, and random error, etc. In addition, according to the satellite precise orbit, the computed satellite-to-receiver range reads:

$$\rho_{sr} = \rho + d_t + d_{sr} + d_{td} + d_{pm} + \epsilon \quad (2)$$

where ρ_{sr} denotes the computed satellite-to-receiver range; $\rho = \sqrt{(x^s - x_r)^2 + (y^s - y_r)^2 + (z^s - z_r)^2}$ with coordinate components of satellite (x^s, y^s, z^s) and receiver (x_r, y_r, z_r) denotes the satellite-to-receiver range; and ϵ mainly contains the residual systematic error [34,35] and random error, which is similar to the observation error in Equation (1). Therefore, the SLR residuals can be obtained as follows:

$$v_{SLR} = \rho_{SLR} - \rho_{sr} \quad (3)$$

where v_{SLR} denotes the SLR residuals to be used in this study.

To make a more comprehensive study on the performance of precise products in this study. The relations between the orbit error and beta angle/elongation angle are analyzed in this study. Figure 1 depicts the geometric space relations among the sun, Earth, and GNSS satellite, where the beta angle and elongation angle are marked. Here, the beta angle represents the elevation angle of the sun above the orbital plane, and the angle between the sun, the satellite, and the Earth is elongation angle [22].

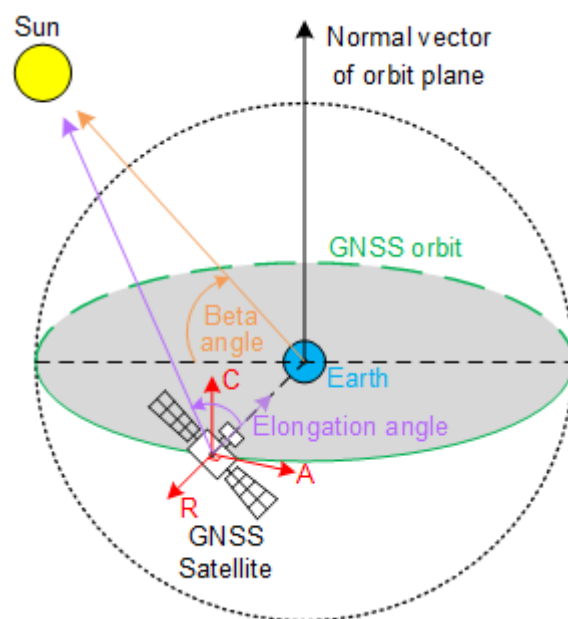


Figure 1. Space geometric angle and position among the sun, Earth, and GNSS satellite.

3. Data and Experiment

In this study, we have compared iGMAS orbits with four MGEX ACs from 10 July 2021 to 10 July 2022 in 366 days. Table 1 summarizes the details of precise orbit products provided by iGMAS, GFZ, ESA, CODE, and WHU. It should be noted that these four ACs were chosen because their products are widely used and include the BDS-3 satellites. The institution, ID, orbit latency, orbit update, orbit sampling, and frequency are all included. It can be seen that the iGMAS has the most extensive range of products.

Table 1. Overview of the orbit products from iGMAS and four MGEX ACs.

Institution	ID	Orbit Latency	Orbit Update	Orbit Sampling	Frequency
iGMAS	ISC	12 days	weekly	15 min	B1I/B3I; B1C/B2a
	ISR	17 h	daily	15 min	B1I/B3I; B1C/B2a
	ISU	3 h	6 h	15 min	B1I/B3I; B1C/B2a
GFZ	GFZ	daily	daily	5 min	B1I/B3I
ESA	ESA	daily	daily	5 min	B1I/B3I
CODE	COD	daily	daily	5 min	B1I/B3I
WHU	WUM	daily	daily	15 min	B1I/B3I

As of July 2022, GFZ, ESA, and CODE are provided BDS orbit with 5-min sampling based B1I/B3I, while WHU and iGMAS orbit products are supplied at 15 min intervals. Figure 2 shows the availability of orbit products from iGMAS and four MGEX ACs. The availability of GFZ, ESA, and COD can reach 100%, while WUM is approximately 92.4%. The ISC, ISR, and ISU products based on B1I/B3I also with high availability, approximately 100%, 99.7%, and 100%, respectively. For the B1C/B2a-based orbit products of iGMAS, the ISC can maintain long-term availability with approximately 91.8%, although interruptions have occurred at some time. In contrast, the availability of ISR and ISU products is much lower than ISC, approximately 14.4%, and 14.5%, respectively. It seems that iGMAS stopped to provide these two products after 27 November 2021. We noticed that iGMAS combined products included all BDS-2 satellites and 27 BDS-3 satellites. Specifically, there are 10 BDS-3 MEO satellites built by SECM, 15 BDS-3 MEO, and 3 BDS-3 IGSO satellites built by CAST.

The PRNs are from C19 to C46, except for the experiment satellite of C31. The satellite products of GFZ and WHU are similar to iGMAS, while BDS-2 GEO satellites are excluded from ESA and CODE products. Note that the time system used in iGMAS products is BDS Time, while MGEX ACs is GPS time (GPST). Therefore, the iGMAS products are converted to GPST compared with the four MGEX ACs. In order to validate the iGMAS product, SLR validation is used in this paper. The SLR observations were collected from the International Laser Ranging Service (ILRS). The other details of the processing strategies are shown in Table 2.

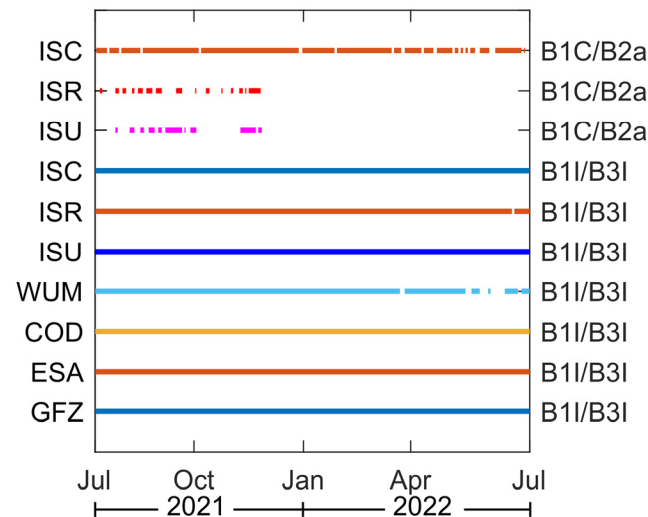


Figure 2. Availability of orbit products from iGMAS and four MGEX ACs.

Table 2. Processing strategies of orbit products.

Item	Strategy
Time Span	DOY 190 in 2021 to DOY 190 in 2022
Orbit compare	iGMAS orbit products convert to GPST and are compared with MGEX ACs BDS-2: all of the GEO, IGSO, and MEO satellites BDS-3: C19–C49 (except C31) BDS-2 GEO: C01 BDS-2 IGSO: C08, C10 BDS-2 MEO: C11 BDS-3 CAST MEO: C20, C21 BDS-3 SCEM MEO: C29, C30
SLR validation	

4. Analysis of Orbit Products

4.1. ISC Products

Figure 3 shows the root mean squares (RMSs) for BDS-2 satellites in along-track, cross-track, and radial directions between iGMAS and MGEX ACs based on B1I/B3I. The BDS-2 GEO satellites are not provided by ESA and CODE. Thus, this paper compares the BDS-2 GEO satellites with GFZ and WHU. As seen in Figure 3, GEO satellites show the most significant RMSs, especially in the along-track direction. Taking the C01 satellite as an example, we can find that the RMS of cross-track between ISC and WHU is much smaller than that of ISC and GFZ. It indicates that the processing strategies of ISC and WHU for GEO satellites may be more similar. For the IGSO satellite, the RMS is at the sub-decimeter to decimeter level between ISC and four MGEX ACs in three directions. For MEO satellites, the RMS is better than GEO and IGSO satellites, especially for the radial direction, which is at the centimeter level. Moreover, the radial accuracy of MEO satellites is much better than both along-track and cross-track directions. This is reasonable because the observations are oriented around the radial direction rather than the along-track and cross-track directions. Overall, the consistency of the BDS-2 GEO orbits between ISC

and WHU products is better than that between ISC and GFZ. For IGSO satellites, CODE showed the best agreement regarding ISC; the RMSs of along-track, cross-track, and radial directions are 0.120 m, 0.113 m, and 0.102 m, respectively. For BDS-2 MEO satellites, ESA showed the best agreement concerning ISC, and the RMSs of along-track, cross-track, and radial directions are 0.102 m, 0.063 m, and 0.051 m, respectively.

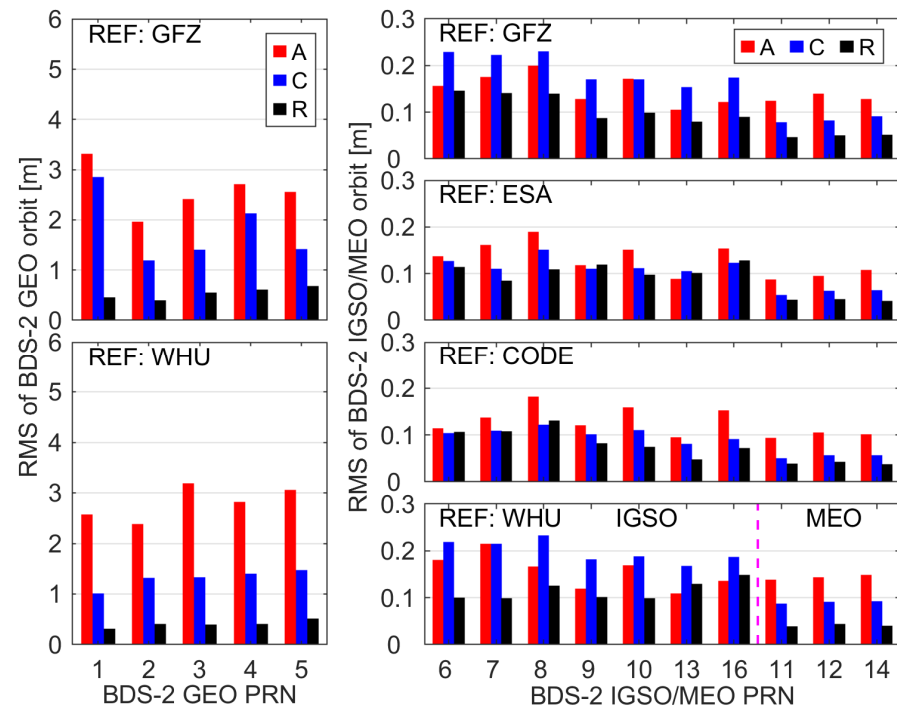


Figure 3. RMS of BDS-2 ISC orbits based on B1I/B3I compared with different MGEX ACs in the along-track (A), cross-track (C), and radial (R) directions, respectively.

Figure 4 shows the RMSs of BDS-3 ISC orbits based on B1I/B3I and B1C/B2a compared with MGEX ACs precise orbit products. The horizontal axis is the RMSs of B1I/B3I and the vertical axis is the RMSs of B1C/B2a. The gray dashed line indicates that the RMSs of B1I/B3I and B1C/B2a are the same. Therefore, the upper part of the dashed line means that B1I/B3I is better than B1C/B2a and vice versa. The circle represents MEO satellites, and the triangle represents IGSO satellites. In addition, different colors are used to distinguish the different directions. That is, the green, blue, and red colors indicate the along-track, cross-track, and radial directions, respectively. As shown in Figure 4, we can see that the comparison results of along-track, cross-track, and radial directions of MEO are basically above the dashed line. This indicates that the consistency of B1C/B2a orbit products is not as good as B1I/B3I. The main reason may be that the phase center offsets and variations corrections for the B1C/B2a orbit are not accurate enough.

Figure 5 shows the box plot of RMSs of ISC orbits based on B1I/B3I and B1C/B2a in along-track, cross-track, and radial directions for SECM MEO, CAST MEO and CAST IGSO satellites. The five short horizontal lines from the top to the bottom of the box chart represent the 100%, 75%, 50%, 25%, and 0% quantiles, respectively. It can be seen that the median values of RMSs of the along-track based on B1I/B3I for SECM MEO, CAST MEO, and CAST IGSO satellites are approximately 0.055 m, 0.050 m, and 0.150 m, respectively. This indicates that the accuracy of SECM MEO satellites is similar to CAST MEO satellites, and both are better than CAST IGSO satellites. However, an extensive variation range of RMS of 0.045 m to 0.072 m can be seen for CAST MEO satellites. This means that the consistency of CAST MEO satellites is not better than SECM MEO satellites. For the cross-track, the median values of RMSs of B1I/B3I for SECM MEO, CAST MEO, and CAST IGSO satellites are approximately 0.042 m, 0.043 m, and 0.137 m, respectively. For the radial

directions, the median values of RMSs of B1I/B3I for SECM MEO, CAST MEO, and CAST IGSO satellites are approximately 0.036 m, 0.038 m, and 0.141 m, respectively.

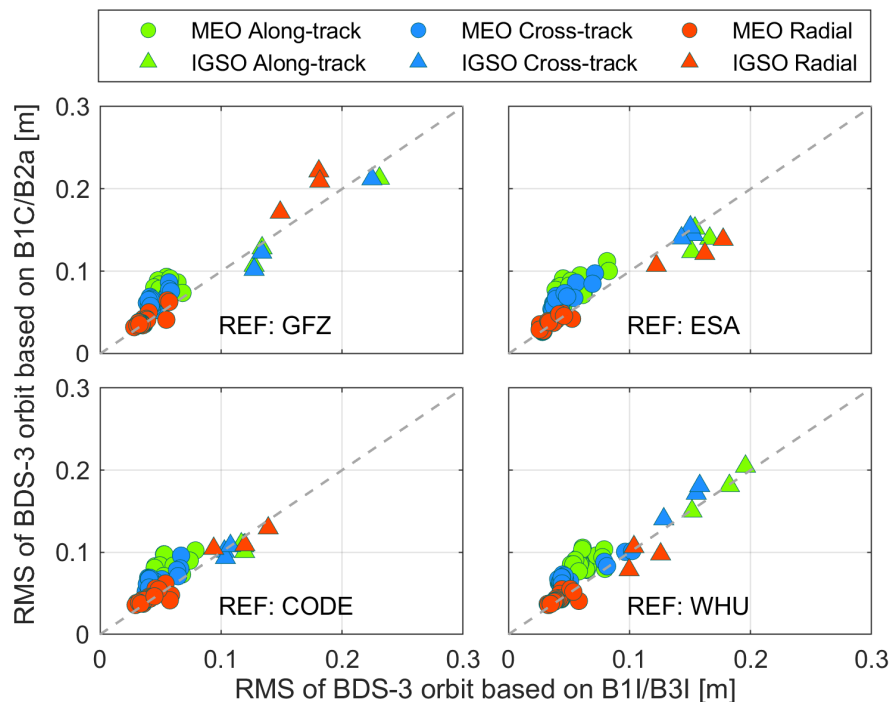


Figure 4. RMS of BDS-3 ISC orbits based on B1I/B3I and B1C/B2a compared with different MGEX ACs in the along-track (A), cross-track (C), and radial (R) directions, respectively.

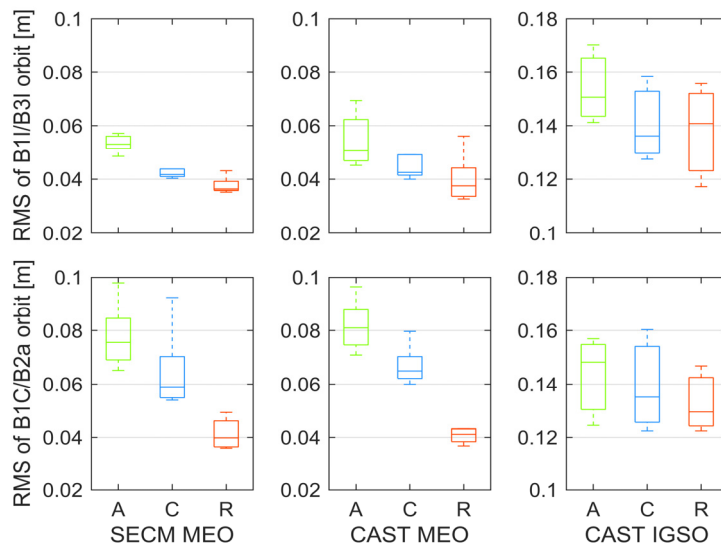


Figure 5. Box plot of RMSs of ISC orbits based on B1I/B3I and B1C/B2a in along-track, cross-track, and radial directions for SECM MEO, CAST MEO, and CAST IGSO satellites, respectively.

4.2. ISR Products

For ISR products, Figure 6 illustrates the RMSs for BDS-2 satellites in along-track, cross-track, and radial directions between ISR B1I/B3I-based and MGEX ACs. We can find that GEO satellites show the largest RMSs in the along-track, cross-track, and radial directions, of which the values are approximately 3.0 m, 1.5 m, and 0.5 m, respectively. For IGSO satellites, the consistency of ISR and MGEX ACs is different. Specifically, the consistency of the cross-track between ISR and ESA/CODE is better than ISR and GFZ/WHU, while the along-track is in contrast. It implies that the different ACs may apply different dynamic

models. For MEO satellites, the consistency of ISR and MGEX ACs is similar. On the other hand, by comparing Figures 3 and 6, we can find that the accuracy of ISR B1I/B3I-based orbits is slightly lower than that of ISC, which is reasonable since the ISC products are the final combined ones.

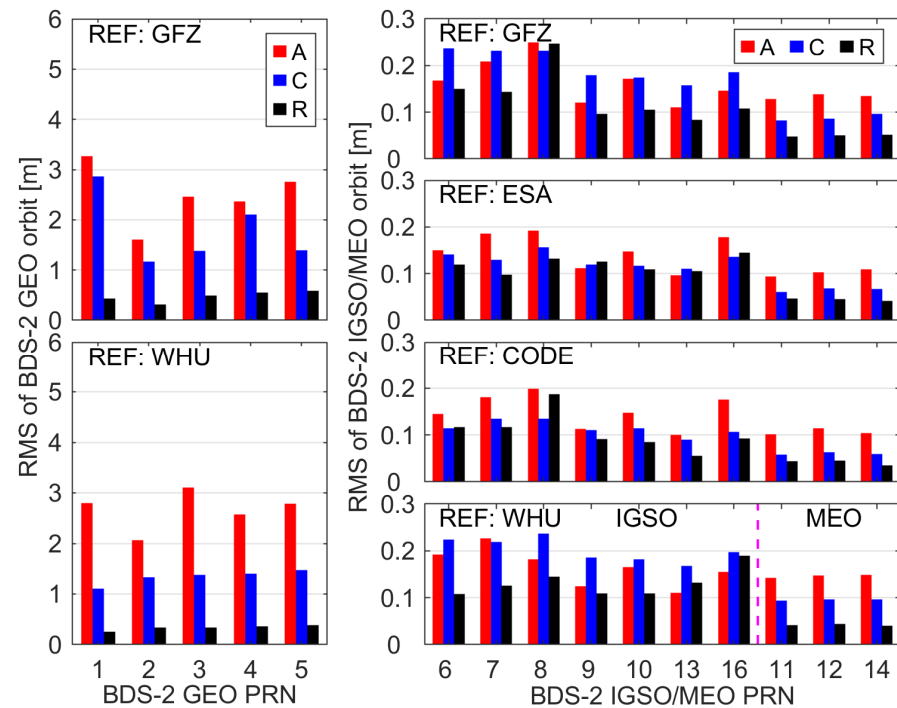


Figure 6. RMS of BDS-2 ISR orbits based on B1I/B3I compared with different MGEX ACs in the along-track (A), cross-track (C), and radial (R) directions, respectively.

To comprehensively assess the difference between ISR B1I/B3I-based and B1C/B2a-based orbit products, Figure 7 shows the comparison results of ISR with four MGEX ACs. Once again, the gray dashed line indicates that the accuracy of ISR B1I/B3I-based and B1C/B2a-based are the same. Thus, the upper part of the dashed line indicates that the accuracy of ISR B1I/B3I-based is better than B1C/B2a-based, and vice versa. We can find that the consistency of ISR B1C/B2a-based orbit products for BDS-3 MEO satellites is worse than B1I/B3I-based. In addition, by comparing Figures 4 and 7, we can find that the orbit accuracy of ISR B1C/B2a-based has decreased compared to ISC, especially for MEO satellites. For the radial directions of BDS-3 IGSO satellites, we can see that the consistency of B1I/B3I-based and B1C/B2a-based for different MGEX ACs is different, and the CODE shows the best consistency with ISR. The reason may be that the processing strategies of ISC and CODE are more consistent than other ACs.

Figure 8 shows the box plot of RMSs of ISR orbits based on B1I/B3I and B1C/B2a in along-track, cross-track, and radial directions for SECM MEO, CAST MEO, and CAST IGSO satellites. As can be seen in Figure 8, the median values of RMSs of the along-track based on B1I/B3I for SECM MEO, CAST MEO, and CAST IGSO satellites are approximately 0.055 m, 0.058 m, 0.175 m, respectively. This demonstrates that the accuracy of SECM MEO satellites is better than CAST MEO satellites in along-track direction. In addition, SECM and CAST MEO satellites are better than CAST IGSO satellites. For the B1C/B2a-based, the median values of RMSs of the along-track for SECM MEO, CAST MEO, and CAST IGSO satellites are approximately 0.085 m, 0.148 m, and 0.164 m, respectively. This means that the consistency of CAST MEO satellites is not better than SECM MEO satellites in along-track direction, and B1C/B2a is significantly different from B1I/B3I. For the cross-track, the median values of RMSs of B1I/B3I for SECM MEO, CAST MEO, and CAST IGSO satellites are approximately 0.042 m, 0.053 m, and 0.153 m, respectively. For the radial directions, the

median values of RMSs of B1I/B3I for SECM MEO, CAST MEO, and CAST IGSO satellites are approximately 0.032 m, 0.037 m, and 0.147 m, respectively.

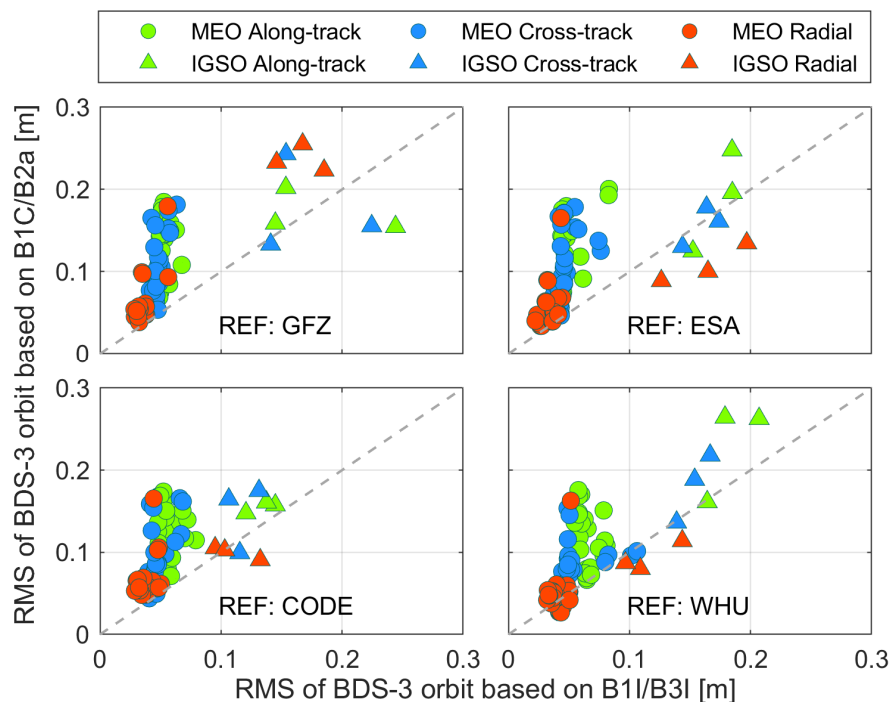


Figure 7. RMS of BDS-3 ISR orbits based on B1I/B3I and B1C/B2a compared with different MGEX ACs in the along-track (A), cross-track (C), and radial (R) directions, respectively.

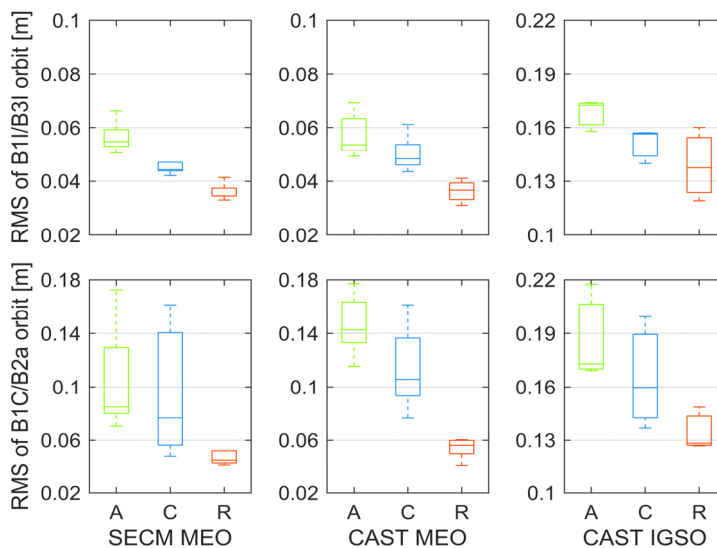


Figure 8. Box plot of RMSs of ISR orbits based on B1I/B3I and B1C/B2a in along-track, cross-track, and radial directions for SECM MEO, CAST MEO, and CAST IGSO satellites, respectively.

4.3. ISU Products

Figure 9 illustrates the RMSs for BDS-2 satellites in along-track, cross-track, and radial directions between ISU B1I/B3I-based and MGEX ACs. It can be clearly seen that the accuracy of ISU becomes much worse, even when compared to WHU. For the along-track direction, the consistency between ISU and GFZ is better than ISU and WHU. However, for the cross-track and radial directions, the consistency of ISU and WHU is better than ISU and GFZ. For IGSO satellites, the consistency of ISU and MGEX ACs is different. That is, the consistency of the cross-track between ISU and ESA/CODE is better than ISU and

GFZ/WHU, while the along-track is in contrast. For MEO satellites, the consistency of ISU and MGEX ACs is similar. Compared with the ISC and ISR products, we can find that the accuracy of ISU products is not as good as others, especially for the BDS-2 GEO satellites.

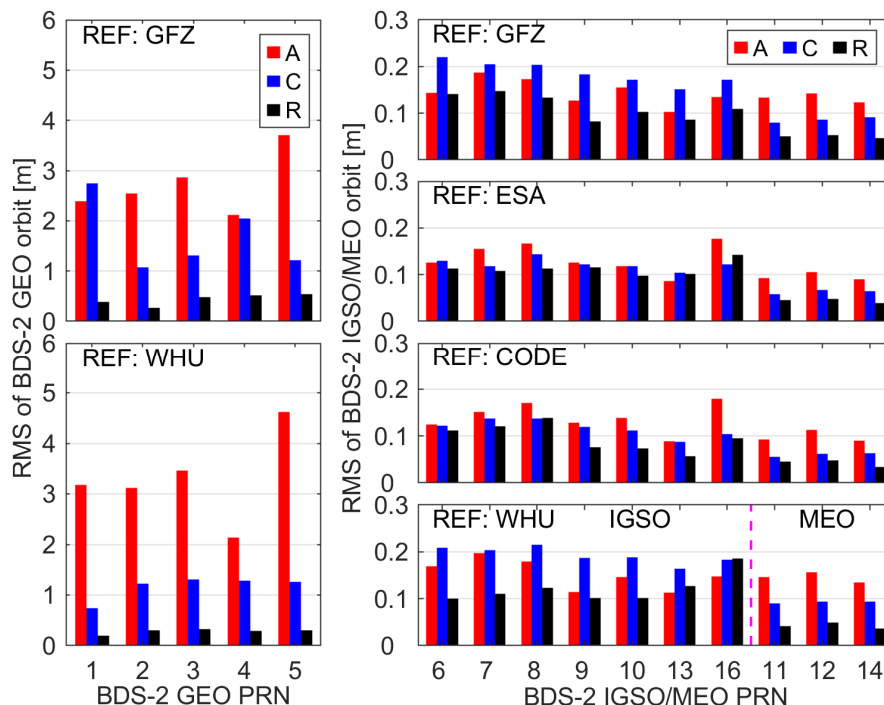


Figure 9. RMS of BDS-2 ISU orbits based on B1I/B3I compared with different MGEX ACs in the along-track (A), cross-track (C), and radial (R) directions, respectively.

Figure 10 shows the RMSs of ISU orbits based on B1I/B3I and B1C/B2a in along-track, cross-track, and radial directions for SECM MEO, CAST MEO, and CAST IGSO satellites, where the gray dashed line indicates that the accuracy of ISU B1I/B3I-based and B1C/B2a-based are the same. We can find that the consistency of ISU B1C/B2a-based orbit products for BDS-3 MEO satellites is worse than B1I/B3I-based. For the radial directions of BDS-3 IGSO satellites, we can see that the consistency of B1I/B3I-based and B1C/B2a-based for different MGEX ACs are different, and the GFZ shows the best consistency with ISU.

Figure 11 shows the box plot of RMSs of ISU orbits based on B1I/B3I and B1C/B2a in along-track, cross-track, and radial directions for SECM MEO, CAST MEO, and CAST IGSO satellites. The five short horizontal lines from the top to the bottom of the box chart represent the 100%, 75%, 50%, 25%, and 0% quantiles, respectively. It can be seen that the median values of RMSs of the along-track based on B1I/B3I for SECM MEO, CAST MEO, and CAST IGSO satellites are approximately 0.061 m, 0.056 m, and 0.146 m, respectively. It indicates that the accuracy of CAST MEO satellites is better than SECM MEO satellites, and both are better than CAST IGSO satellites. However, an extensive variation range of RMS of 0.052 m to 0.075 m can be seen for CAST MEO satellites. This means that the consistency of some CAST MEO satellites is not better than SECM MEO satellites in ISU products. For the B1C/B2a-based, the median values of RMSs of the along-track for SECM MEO, CAST MEO, and CAST IGSO satellites are approximately 0.076 m, 0.136 m, and 0.124 m, respectively. This means that the consistency of CAST MEO satellites is not better than SECM MEO satellites, and B1C/B2a is significantly different from B1I/B3I. For the cross-track, the median values of RMSs of B1I/B3I for SECM MEO, CAST MEO, and CAST IGSO satellites are approximately 0.045 m, 0.096 m, and 0.140 m, respectively. For the radial directions, the median values of RMSs of B1I/B3I for SECM MEO, CAST MEO, and CAST IGSO satellites are approximately 0.041, 0.052, and 0.104 m, respectively.

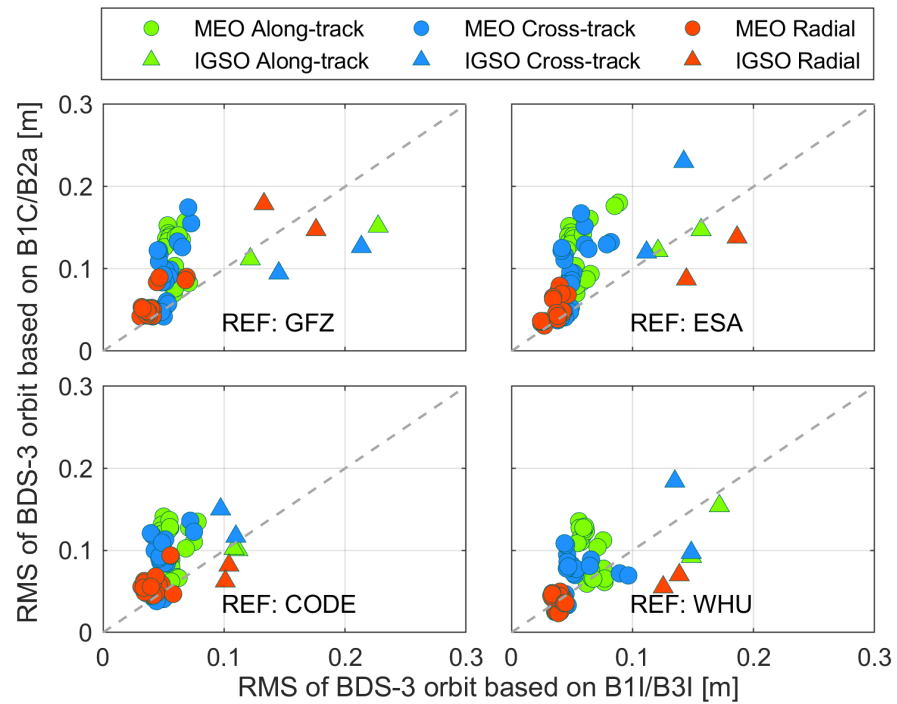


Figure 10. RMS of BDS-3 ISU orbits based on B1I/B3I and B1C/B2a compared with different MGEX ACs in the along-track (A), cross-track (C), and radial (R) directions, respectively.

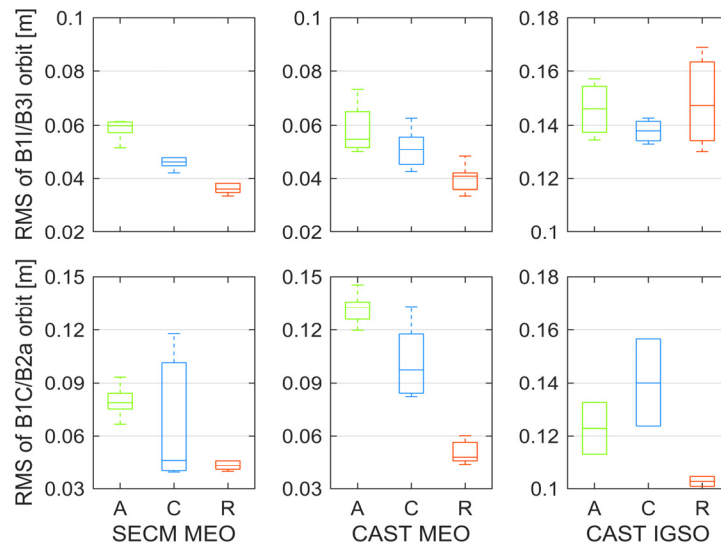


Figure 11. Box plot of RMSs of ISU orbits based on B1I/B3I and B1C/B2a in along-track, cross-track, and radial directions for SECM MEO, CAST MEO, and CAST IGSO satellites, respectively.

5. Inspection with SLR Residuals

5.1. B1I/B3I Frequencies

The SLR technique measures the distance from the SLR station to the laser retroreflector arrays of the satellite. This distance can also be calculated using satellite and station coordinates. The SLR residuals are the difference between the observed and computed distance and are traditionally used as an external inspection of GNSS satellite orbits. Figure 12 shows the SLR residuals for the BDS-2 GEO (C01), IGSO (C08 and C10), and MEO (C11) satellites in the iGMAS ISC, ISR, and ISU B1I/B3I-based orbit products from 10 July 2021 to 10 July 2022. The panels from top to bottom denote the SLR residuals of different satellites. It is worth noting that the residuals with absolute values larger than

1.5 m, 0.5 m, and 0.5 m were removed as outliers for the GEO, IGSO, and MEO satellites in this study. We can find that the GEO and IGSO satellites almost have a systematic bias of approximately 0.3 m. In addition, the performance of C11 is better than that of C01, C08, and C10, which is possibly attributed to the better geometry condition of MEO satellites. The panels from left to right denote the SLR residuals of ISC, ISR, and ISU products. It can be found that for the same satellite, the SLR residuals have similar behaviors to some extent, but some differences can also be found. Specifically, the magnitude of the fluctuations of the SLR residuals is different for ISC, ISR, and ISU products, where the ISC product is the best.

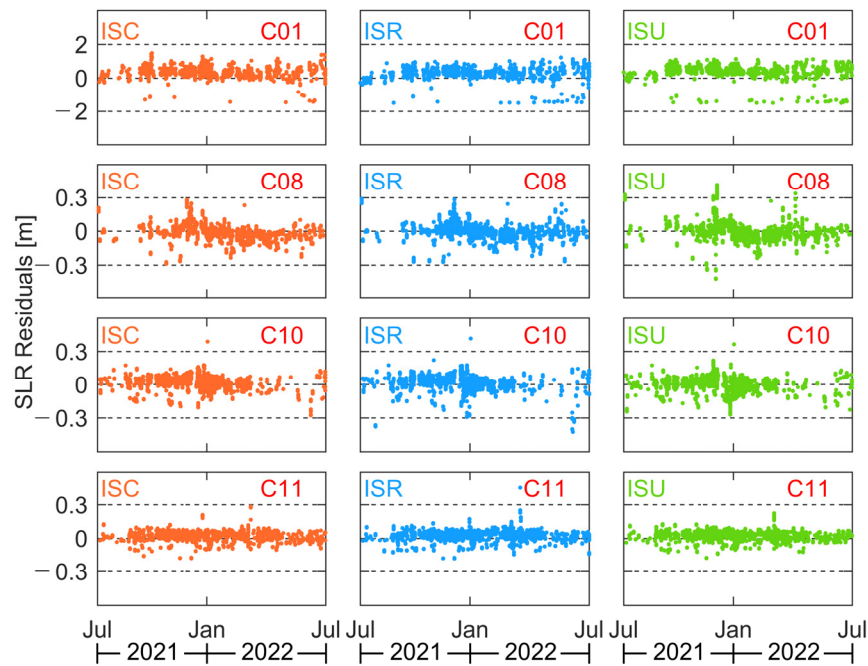


Figure 12. SLR residuals of BDS-2 satellites based on three types of iGMAS B1I/B3I orbits.

Figure 13 shows the SLR residuals for the BDS-3 CAST MEO (C20 and C21) and SECM MEO (C29 and C30) satellites in the iGMAS ISC, ISR, and ISU B1I/B3I-based orbit products from 10 July 2021 to 10 July 2022. The SLR residuals show significant changes in these periods. After the detection and removal of outliers in the SLR observations, there are 2795 normal points available for C20, 2702 for C21, 2483 for C29, and 2528 for C30. First of all, compared with Figure 12, the amplitudes of residuals in Figure 13 are smaller than the ones in Figure 12, thus indicating that the accuracy of precise orbits of BDS-3 is better than that of BDS-2. The mean values are 3.49 cm, 3.36 cm, -2.52 cm, and -2.16 cm for C20, C21, C29, and C30, respectively. It indicates a systematic error in the SLR residuals of the CAST MEO and SECM MEO satellites; one is generally positive, and the other is negative. This phenomenon may be related to the manufacturer, which can be considered for modeling in the future. In addition, the SLR residuals are obviously abnormal over a period of time. The main reason is that the force models are not accurate enough when satellites enter the eclipse period.

5.2. B1C/B2a Frequencies

Figure 14 shows the SLR residuals for the BDS-3 CAST MEO (C20 and C21) and SECM MEO (C29 and C30) satellites in the iGMAS ISC, ISR, and ISU B1C/B2a-based orbit products from 10 July 2021 to 10 July 2022. It can be found that the performance of C20 and C21 is better than that of C29 and C30. The panels from left to right denote the SLR residuals of ISC, ISR, and ISU products. It can be seen that for the same satellite, the SLR residuals have similar behaviors to some extent, but some differences can also be found. Specifically, the missing SLR residual data for ISR and ISU are more significant mainly

because there is no corresponding orbit product. Taking a closer look at Figure 14, the accuracy of precise orbits based on B1C/B2a frequencies is generally worse than that of B1I/B3I frequencies. Specifically, the STD values of ISC/ISR/ISU for CAST MEO (C20 and C21) and SECM MEO (C29 and C30) satellites are approximately 0.058/0.088/0.089 m, and 0.065/0.067/0.051 m, respectively.

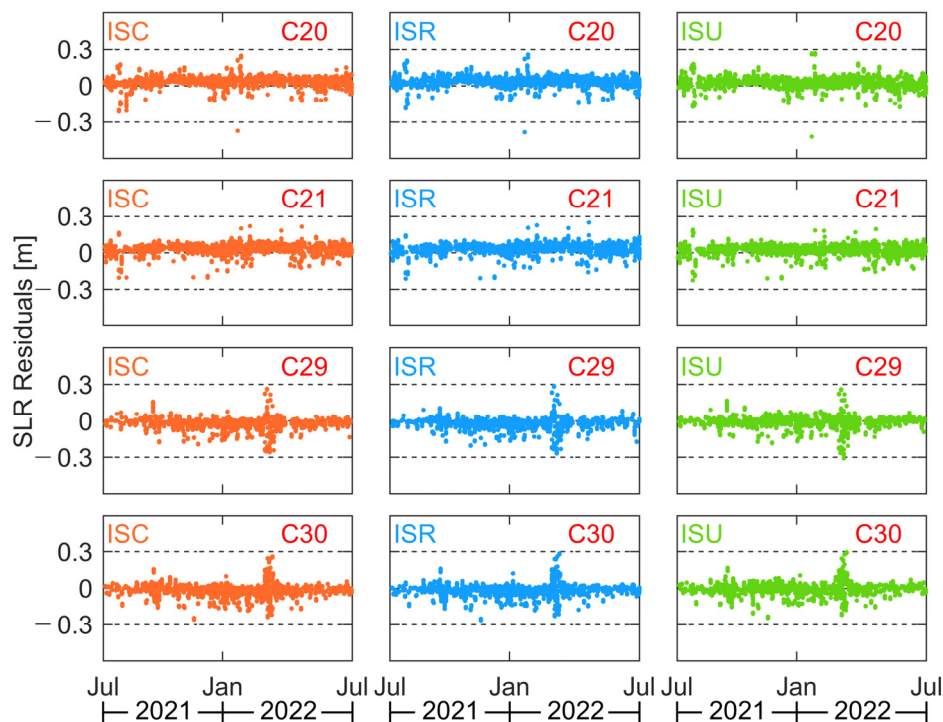


Figure 13. SLR residuals of BDS-3 satellites based on three types of iGMAS B1I/B3I orbits.

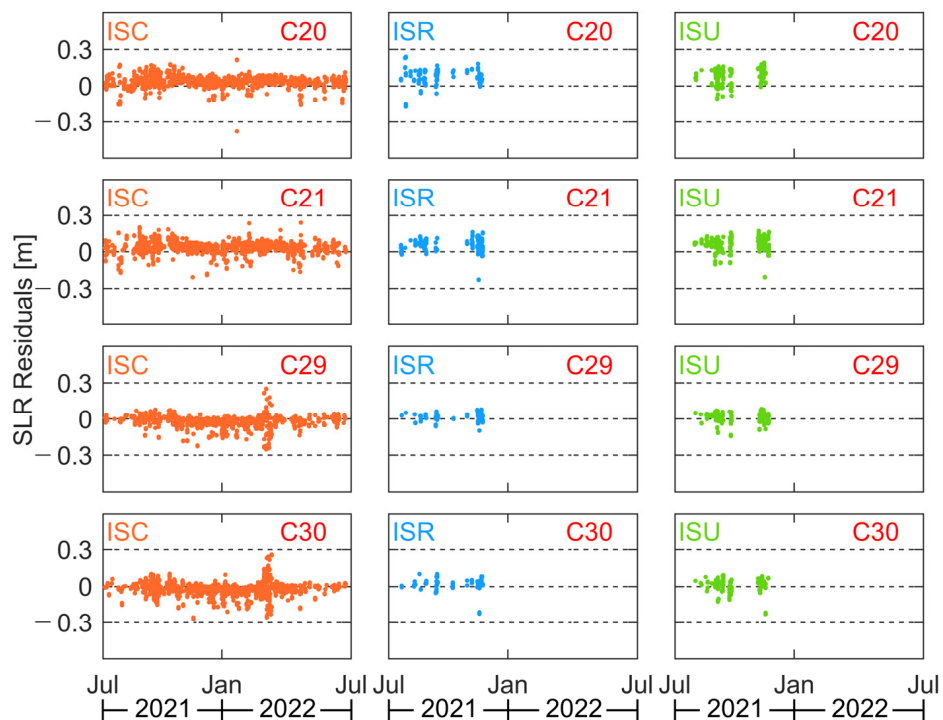


Figure 14. SLR residuals of BDS-3 satellites based on three types of iGMAS B1C/B2a orbits.

6. Discussion of Orbit Errors

6.1. Beta Angle

Figure 15 illustrates the relationship between SLR residuals and beta angle. The panels from top to bottom are the results of BDS-2 GEO (C01), IGSO (C08 and C10), and MEO (C11) satellites. The orange, blue, and green scatters represent the SLR residuals of ISC, ISR, and ISU orbits, respectively. The grey-shaded area in Figure 15 represents the eclipse period, and the rest are non-eclipse periods. As shown in Figure 15, we can find that the beta angle ranges approximately from -49 to $+49$ degrees for IGSO, -33 to 33 degrees for MEO, and from -23 to $+23$ degrees for GEO, respectively. The RMS of SLR residuals for C01 of ISC, ISR, and ISU orbits in the non-eclipse/eclipse periods are $0.473/0.455$ m, $0.480/0.458$ m, and $0.597/0.533$ m, respectively. One of the main reasons for the poor accuracy of GEO satellites is that there is little change in the geometry of the satellite and the station. In addition, it is noteworthy that the SLR residuals of the GEO satellite in eclipse period are better than non-eclipse period, which indicates the apparent deficiency of the non-conservative force model. For the IGSO satellites, The RMS of SLR residuals in the non-eclipse/eclipse periods are approximately $0.056\text{--}0.066/0.084\text{--}0.112$ m; the accuracy decreased by approximately 30% in the eclipse period. It implies that IGSO behaves inconsistently with GEO after entering the eclipse periods. For the BDS-2 MEO satellite, the SLR residuals in the non-eclipse/eclipse periods are approximately $0.044\text{--}0.049/0.050\text{--}0.056$ m; the accuracy decreased by approximately 12% in the eclipse period. It is clear that IGSO/MEO has a similar phenomenon when entering the eclipse periods.

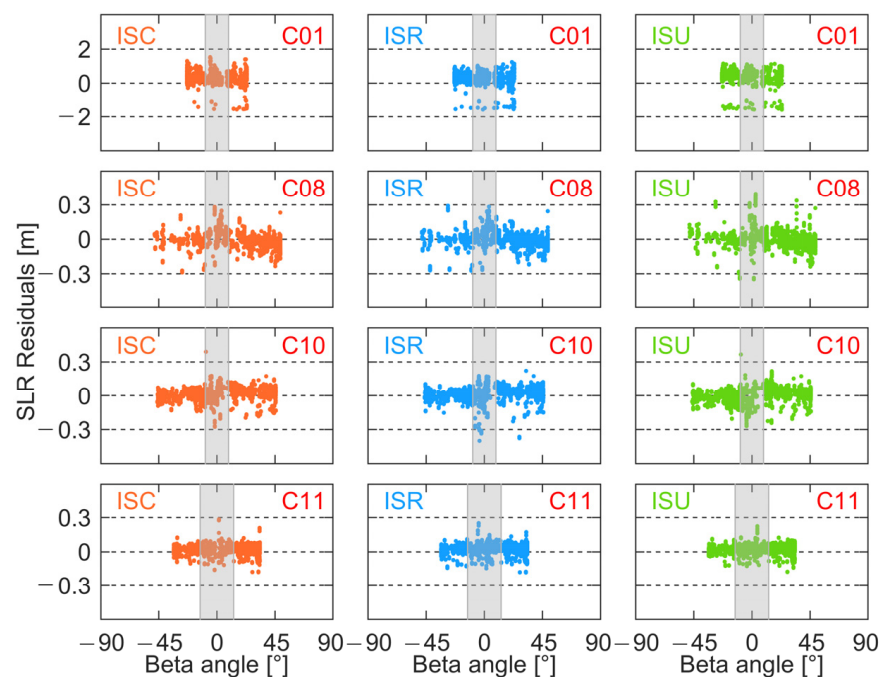


Figure 15. SLR residuals of BDS-2 satellites based on three types of iGMAS B1I/B3I orbits versus beta angle.

Figures 16 and 17 show the relationship between SLR residuals and beta angle for B1I/B3I-based and B1C/B2a-based orbits, respectively. From Figures 16 and 17, we can find that the characteristics of satellites produced by the same manufacturer are more similar. The beta angle ranges from -68 to $+68$ degrees for CAST MEO satellites (C20 and C21) and -32 to $+32$ degrees for SECM MEO satellites (C29 and C30). Figure 16 shows that the RMS of SLR residuals for CAST MEO satellites in the non-eclipse/eclipse periods are approximately $0.049/0.068$ m, while the SECM MEO satellites are approximately $0.045/0.068$ m. Obviously, the accuracy of both BDS-3 CAST MEO and SECM MEO satellites is similar, and both decrease in accuracy after entering the eclipse periods by approximately

33%. Due to the low availability of ISR and ISU products and the low volume of data during the eclipse period, only the ISC products for B1C/B2a were compared.

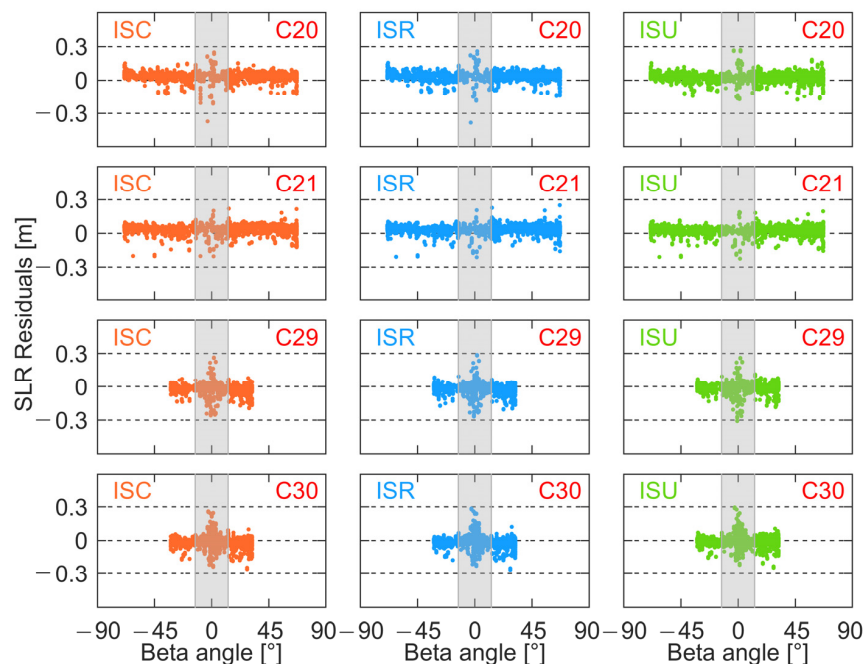


Figure 16. SLR residuals of BDS-3 satellites based on three types of iGMAS B1I/B3I orbits versus beta angle.

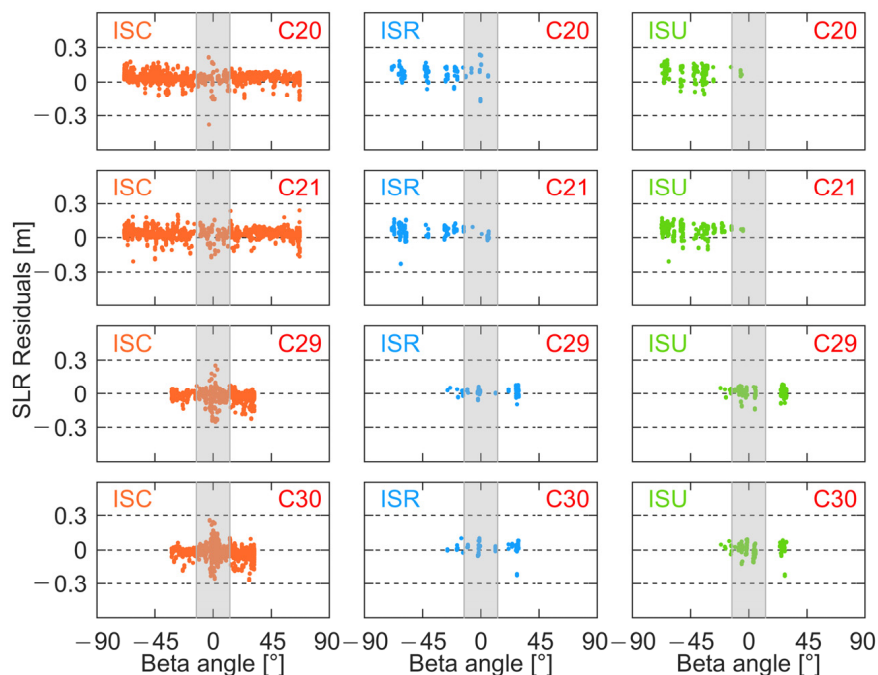


Figure 17. SLR residuals of BDS-3 satellites based on three types of iGMAS B1C/B2a orbits versus beta angle.

6.2. Elongation Angle

Figure 18 shows the relationship between SLR residuals for ISC, ISR, and ISU orbits of BDS-2 GEO (C01), IGSO (C08 and C10), MEO (C11) satellites, and the satellite–sun elongation angle. Once again, the orange, blue, and green scatters represent the SLR residuals of ISC, ISR, and ISU orbits, respectively. The purple line represents the linear

function of the satellite laser residuals concerning the elongation angle. We can find that the elongation angle range for C01 is approximately from 1 to 117 degrees and shows a strong correlation with the SLR residuals as the elongation angle increases. The slopes of ISC/ISR/ISU orbit are approximately 0.1627/0.1982/0.0843 cm/°. In addition, We can find that C01 in ISU obviously has unmodeled error. The reason may be that the GEO observation conditions are poor and the force models are not accurate enough. Moreover, the ISU orbits are generated without a higher precision initial orbit, which is generally worse than ISR and ISC orbits. For the IGSO satellites, C08 and C10 have different characteristics from C01. Specifically, the range of elongation angle for IGSO is approximately 1 to 143 degrees, which is more significant than C01. In addition, their SLR residuals are negatively correlated with the elongation angle. The SLR residuals of IGSO satellites are mostly negative when the elongation angle is close to 140° and positive when the elongation angle is close to 0°. This systematic error may be due to the fact that the surface area of the Z surface of the satellite is much smaller than the X surface area and the higher-order solar radiation pressure (SRP) uptake term is not yet well modeled. For the MEO satellite, C11 has the most extensive elongation angle range, approximately from 2 to 163 degrees, and has the most minor linear correlation with SLR residuals. Thus, this indicates that the SLR residuals exhibit systematic error characteristics related to the type of satellite. The non-conservative force models such as SRP may not be suitable for all satellites. Therefore, building a more accurate non-conservative force model may be one of the ways to weaken the systematic errors of SLR for iGMAS orbit products.

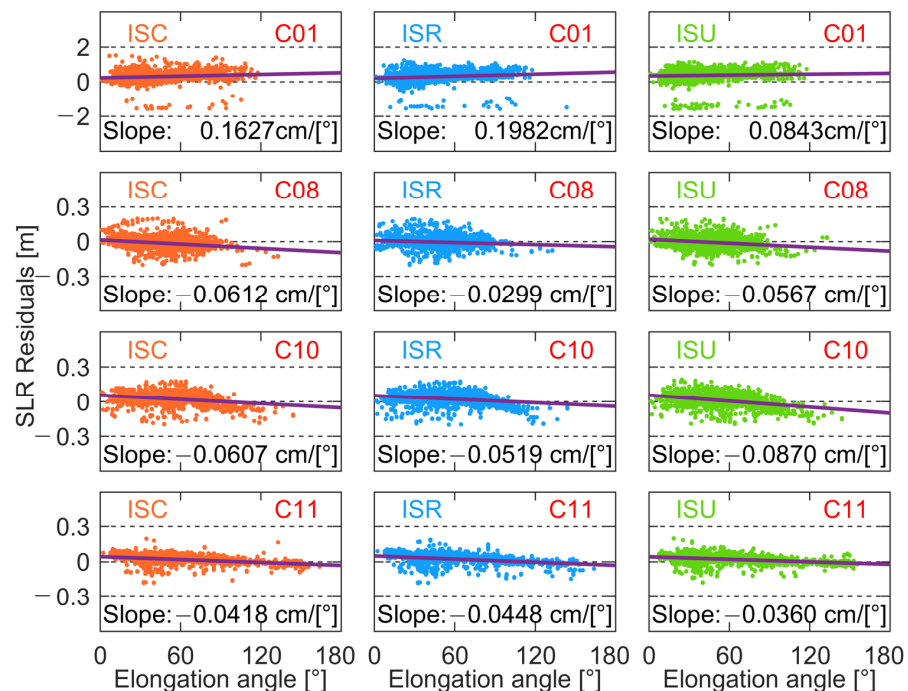


Figure 18. SLR residuals of BDS-2 satellites based on three types of iGMAS B1I/B3I orbits versus elongation angle.

Figures 19 and 20 show the relationship between SLR residuals and elongation angle for B1I/B3I-based and B1C/B2a-based orbits, respectively. Figures 19 and 20 show that the elongation angle range for CAST MEO and SECM MEO satellites is similar to BDS-2 MEO satellites, approximately from 2 to 163 degrees. We note that all elongation angles are more significant than 0 degrees. This is because the sun–satellite–Earth is co-linear, and SLR observations are unavailable. Judging from Figure 19, we can find the slope for C20 of ISC/ISR/ISU orbit is approximately $-0.0156/-0.0131/0.011$ cm/°, and for the other CAST MEO satellite C21, the slope has similar characteristics, with positive ISC/ISR and negative ISU. The main reasons are the insignificant degree of linear correlation, and the

data period is not very long. For SECM MEO satellites, the slopes of C29 and C30 are both positive and more significant than CAST MEO satellites. Figure 20 shows that the SLR residuals of the ISC B1C/B2a-based orbits are similar to the B1I/B3I-based orbits, with no significant systematic errors. However, the SLR residuals of the ISR/ISU B1C/B2a-based orbits show a strong linear relationship with the elongation angle, mainly due to the large fitting error caused by insufficient data.

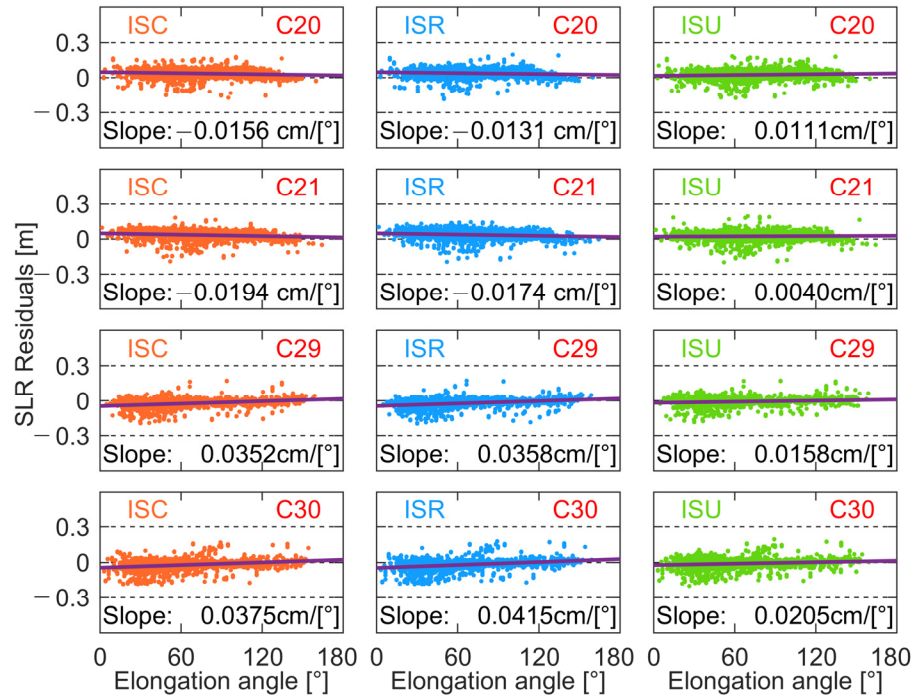


Figure 19. SLR residuals of BDS-3 satellites based on three types of iGMAS B1I/B3I orbits versus elongation angle.

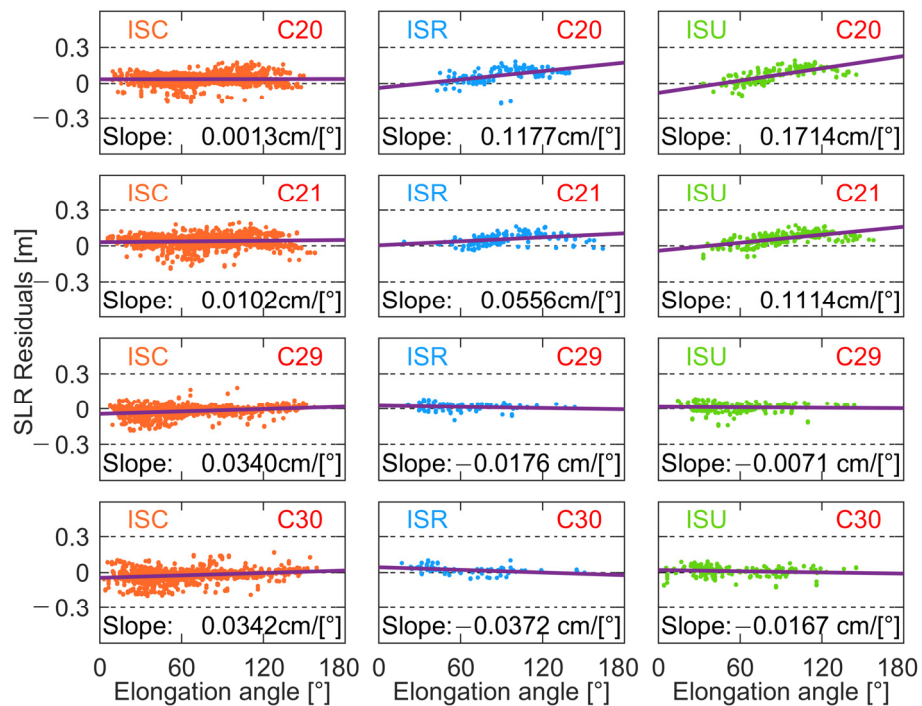


Figure 20. SLR residuals of BDS-3 satellites based on three types of iGMAS B1C/B2a orbits versus elongation angle.

7. Conclusions

In this paper, three kinds of precise orbit, i.e., ISC, ISR, and ISU products, are comprehensively assessed, where the BDS-2/BDS-3 based on B1I/B3I and B1C/B2a frequencies are all considered. The main conclusions can be made based on one year of iGMAS data and other supplementary data, including four precise orbits of four ACs and SLR data. Several main conclusions can be made.

Considering the orbit accuracy according to the four ACs, for the ISC products based on B1I/B3I frequencies, GEO satellites show the most significant biases. The accuracy of IGSO satellites is sub-decimeter level to decimeter level. Then, the accuracy for MEO satellites in three directions can reach the centimeter level, especially the radial direction. Additionally, the consistency of B1C/B2a orbit products is not as good as B1I/B3I. In the future, there is room for improvement in B1C/B2a-based products. Similar conclusions can be found for the ISR products, and the accuracy of B1I/B3I-based ISR products is slightly lower than that of ISC, which is reasonable since the ISC products are the final combined ones. For the ISU products, the accuracy becomes much worse than the other two products, especially for the BDS-2 GEO satellites.

By using the SLR technique, the precise orbits are inspected. For the B1I/B3I frequencies, the BDS-2 GEO and IGSO satellites have a systematic bias of approximately 0.3 m, whereas the BDS-2 MEO satellites do not display this. The accuracy of precise orbits of BDS-3 are better than those of BDS-2. Specifically, the mean values are 3.49 cm, 3.36 cm, −2.52 cm, and −2.16 cm for C20, C21, C29, and C30, respectively. Comparing three types of orbit products, the ISC product has the best performance. Additionally, we find that the orbit errors are related to the manufacturer, which can be considered for modeling in the future. For the B1C/B2a frequencies, similar conclusions can be found. Then, the accuracy of precise orbits based on B1C/B2a frequencies is generally worse than that of B1I/B3I frequencies. Specifically, the mean STD values of ISC/ISR/ISU for CAST MEO and SECM MEO satellites are approximately 0.078 m and 0.061 m, respectively.

When analyzing the impact factors of orbit errors, the results show that they are related to the beta angle and elongation angle. Specifically, for the beta angle, the BDS-2 GEO satellites are more accurate in the eclipse period, mainly due to the deficiency of the non-conservative force model. At the same time, the accuracy of the precise orbits in the non-eclipse period is better in BDS-2/BDS-3 IGSO and MEO satellites. For the elongation angle, there is a strong positive correlation with the SLR residuals for BDS-2 GEO satellites, whereas negative correlations can be found for BDS-2 IGSO and MEO satellites. This indicates that the non-conservative force models such as SRP may not be suitable for all satellites. Then, for the BDS-3 MEO satellites, the behaviors in terms of elongation angle are similar to the BDS-2 MEO satellites. It is worth noting that, compared with the behaviors of B1I/B3I frequencies, the B1C/B2a frequencies are different, especially for the ISR/ISU products, where a strong linear relationship exists with the elongation angle. Unlike the beta angle, the impacts of the elongation angle are related to the manufacturer.

Author Contributions: Conceptualization, Z.Z. and Y.W.; methodology, Z.Z. and P.Z.; software, L.H. and P.Z.; validation, Y.W., L.H. and X.H.; data Curation, Z.Z. and P.Z.; writing—original draft preparation, Z.Z. and P.Z.; writing—review and editing, Z.Z. and P.Z. All authors have read and agreed to the published version of the manuscript.

Funding: This study is partly supported by the National Natural Science Foundation of China (42004014), the Natural Science Foundation of Jiangsu Province (BK20200530), and the National Natural Science Foundation of China (41974001).

Data Availability Statement: The datasets analyzed in this study are managed by the School of Earth Sciences and Engineering, Hohai University, and can be available upon reasonable request from the corresponding author.

Acknowledgments: The authors thank the iGMAS, IGS, MGEX, and ILRS authorities for providing the data for this study.

Conflicts of Interest: The authors have no relevant financial or non-financial interest to disclose.

References

1. Yang, Y.; Mao, Y.; Sun, B. Basic Performance and Future Developments of BeiDou Global Navigation Satellite System. *Satell. Navig.* **2020**, *1*, 1. [[CrossRef](#)]
2. Yang, Y.; Gao, W.; Guo, S.; Mao, Y.; Yang, Y. Introduction to BeiDou-3 Navigation Satellite System. *Navigation* **2019**, *66*, 7–18. [[CrossRef](#)]
3. CSNO *BeiDou Navigation Satellite System Signal in Space Interface Control Document Open Service Signal B1C (Version 1.0)*; China Satellite Navigation Office: Beijing, China, 2017.
4. CSNO *BeiDou Navigation Satellite System Signal in Space Interface Control Document Open Service Signal B2a (Version 1.0)*; China Satellite Navigation Office: Beijing, China, 2017.
5. CSNO *BeiDou Navigation Satellite System Signal in Space Interface Control Document Open Service Signal B3I (Version 1.0)*; China Satellite Navigation Office: Beijing, China, 2018.
6. CSNO *BeiDou Navigation Satellite System Signal in Space Interface Control Document Open Service Signal B1I (Version 3.0)*; China Satellite Navigation Office: Beijing, China, 2019.
7. CSNO *BeiDou Navigation Satellite System Signal in Space Interface Control Document Open Service Signal B2b (Version 1.0)*; China Satellite Navigation Office: Beijing, China, 2020.
8. CSNO. Fundamental PNT Service. 2022. Available online: <http://www.csno-tarc.cn/en/system/constellation> (accessed on 1 December 2022).
9. Zhao, Q.; Guo, J.; Wang, C.; Lyu, Y.; Xu, X.; Yang, C.; Li, J. Precise Orbit Determination for BDS Satellites. *Satell. Navig.* **2022**, *3*, 2. [[CrossRef](#)]
10. Kouba, J. *A Guide to Using International GNSS Service (IGS) Products*; Maryland Biological Stream Survey; Versar, Inc.: Springfield, VA, USA, 2009; Volume 4, p. 106.
11. IGS. IGS Analysis Centers. 2022. Available online: <https://igs.org/acc/#ac-list> (accessed on 1 December 2022).
12. Montenbruck, O.; Steigenberger, P.; Prange, L.; Deng, Z.; Zhao, Q.; Perosanz, F.; Romero, I.; Noll, C.; Stürze, A.; Weber, G.; et al. The Multi-GNSS Experiment (MGEX) of the International GNSS Service (IGS)—Achievements, Prospects and Challenges. *Adv. Space Res.* **2017**, *59*, 1671–1697. [[CrossRef](#)]
13. Montenbruck, O.; Steigenberger, P.; Khachikyan, R.; Weber, G.; Langley, R.; Mervart, L.; Hugentobler, U. IGS-MGEX: Preparing the Ground for Multi-Constellation GNSS Science. *Inside GNSS* **2014**, *9*, 42–49.
14. Ai, Q.; Maciuk, K.; Lewinska, P.; Borowski, L. Characteristics of Onefold Clocks of GPS, Galileo, BeiDou and GLONASS Systems. *Sensors* **2021**, *21*, 2396. [[CrossRef](#)] [[PubMed](#)]
15. Jadászliwer, B.; Camparo, J. Past, Present and Future of Atomic Clocks for GNSS. *GPS Solut.* **2021**, *25*, 27. [[CrossRef](#)]
16. Chen, Q.; Song, S.; Zhou, W. Accuracy Analysis of GNSS Hourly Ultra-Rapid Orbit and Clock Products from SHAO AC of IGMAS. *Remote Sens.* **2021**, *13*, 1022. [[CrossRef](#)]
17. Kazmierski, K.; Zajdel, R.; Sośnica, K. Evolution of Orbit and Clock Quality for Real-Time Multi-GNSS Solutions. *GPS Solut.* **2020**, *24*, 111. [[CrossRef](#)]
18. Zhou, W.; Cai, H.; Chen, G.; Jiao, W.; He, Q.; Yang, Y. Multi-GNSS Combined Orbit and Clock Solutions at IGMAS. *Sensors* **2022**, *22*, 457. [[CrossRef](#)]
19. Jiao, W.; Ding, Q.; Li, J.; Lu, X.; Feng, L.; Ma, J.; Chen, G. Monitoring and Assessment of GNSS Open Services. *J. Navig.* **2011**, *64*, S19–S29. [[CrossRef](#)]
20. Cai, H.; Chen, K.; Xu, T.; Chen, G. The IGMAS Combined Products and the Analysis of Their Consistency. In Proceedings of the China Satellite Navigation Conference (CSNC) 2015 Proceedings, Xi’an, China, 13–15 May 2015; Springer: Berlin/Heidelberg, Germany, 2015; Volume III, pp. 213–226.
21. iGMAS. Analysis Centers. 2022. Available online: http://en.igmas.org/About/Showigmas/detail/nav_id/6/cate_id/62.html (accessed on 1 December 2022).
22. Ye, F.; Yuan, Y.; Yang, Z. Validation and Evaluation on B1I/B3I-Based and B1C/B2a-Based BDS-3 Precise Orbits from IGMAS. *Adv. Space Res.* **2022**, *70*, 2167–2177. [[CrossRef](#)]
23. Ye, F.; Yuan, Y.; Deng, Z. Improved Ultra-Rapid UT1-UTC Determination and Its Preliminary Impact on GNSS Satellite Ultra-Rapid Orbit Determination. *Remote Sens.* **2020**, *12*, 3584. [[CrossRef](#)]
24. Li, Z.; Wang, N.; Wang, L.; Liu, A.; Yuan, H.; Zhang, K. Regional Ionospheric TEC Modeling Based on a Two-Layer Spherical Harmonic Approximation for Real-Time Single-Frequency PPP. *J. Geod.* **2019**, *93*, 1659–1671. [[CrossRef](#)]
25. Li, X.; Chen, X.; Ge, M.; Schuh, H. Improving Multi-GNSS Ultra-Rapid Orbit Determination for Real-Time Precise Point Positioning. *J. Geod.* **2019**, *93*, 45–64. [[CrossRef](#)]
26. Chen, K.; Xu, T.; Chen, G.; Li, J.; Yu, S. The Orbit and Clock Combination of IGMAS Analysis Centers and the Analysis of Their Precision. In Proceedings of the China Satellite Navigation Conference (CSNC) 2015 Proceedings, Xi’an, China, 13–15 May 2015; Springer: Berlin/Heidelberg, Germany, 2015; Volume II, pp. 421–438.
27. Tan, B.; Yuan, Y.; Wen, M.; Ning, Y.; Liu, X. Initial Results of the Precise Orbit Determination for the New-Generation BeiDou Satellites (BeiDou-3) Based on the IGMAS Network. *ISPRS Int. J. Geo-Inf.* **2016**, *5*, 196. [[CrossRef](#)]

28. Zhang, X.; Li, X.; Lu, C.; Wu, M.; Pan, L. A Comprehensive Analysis of Satellite-Induced Code Bias for BDS-3 Satellites and Signals. *Adv. Space Res.* **2019**, *63*, 2822–2835. [[CrossRef](#)]
29. Li, X.; Xie, W.; Huang, J.; Ma, T.; Zhang, X.; Yuan, Y. Estimation and Analysis of Differential Code Biases for BDS3/BDS2 Using IGMAS and MGEX Observations. *J. Geod.* **2019**, *93*, 419–435. [[CrossRef](#)]
30. Xie, X.; Fang, R.; Geng, T.; Wang, G.; Zhao, Q.; Liu, J. Characterization of GNSS Signals Tracked by the IGMAS Network Considering Recent BDS-3 Satellites. *Remote Sens.* **2018**, *10*, 1736. [[CrossRef](#)]
31. Yang, H.; Xu, T.; Nie, W.; Gao, F.; Guan, M. SLR Validation and Evaluation on BDS Precise Orbits from 2013 to 2018. *Adv. Space Res.* **2019**, *64*, 475–490. [[CrossRef](#)]
32. Montenbruck, O.; Steigenberger, P.; Wang, N.; Hauschild, A. Characterization and Performance Assessment of BeiDou-2 and BeiDou-3 Satellite Group Delays. *NAVIGATION J. Inst. Navig.* **2022**, *69*, navi.526. [[CrossRef](#)]
33. Arnold, D.; Montenbruck, O.; Hackel, S.; Sośnica, K. Satellite Laser Ranging to Low Earth Orbiters: Orbit and Network Validation. *J. Geod.* **2019**, *93*, 2315–2334. [[CrossRef](#)]
34. Zhang, Z.; Li, B.; Shen, Y.; Gao, Y.; Wang, M. Site-Specific Unmodeled Error Mitigation for GNSS Positioning in Urban Environments Using a Real-Time Adaptive Weighting Model. *Remote Sens.* **2018**, *10*, 1157. [[CrossRef](#)]
35. Zhang, Z.; Li, B. Unmodeled Error Mitigation for Single-Frequency Multi-GNSS Precise Positioning Based on Multi-Epoch Partial Parameterization. *Meas. Sci. Technol.* **2020**, *31*, 025008. [[CrossRef](#)]

Disclaimer/Publisher’s Note: The statements, opinions and data contained in all publications are solely those of the individual author(s) and contributor(s) and not of MDPI and/or the editor(s). MDPI and/or the editor(s) disclaim responsibility for any injury to people or property resulting from any ideas, methods, instructions or products referred to in the content.